

NRC Publications Archive Archives des publications du CNRC

Consensus Standards for acquisition, measurement, and reporting of intravascular optical coherence tomography studies

Tearney, Guillermo J.; Regar, Evelyn; Akasaka, Takashi; Adriaenssens, Tom; Barlis, Peter; Bezerra, Hiram G.; Bouma, Brett; Bruining, Nico; Cho, Jin-man; Chowdhary, Saqib; Costa, Marco A.; De Silva, Ranil; Dijkstra, Jouke; Di Mario, Carlo; Dudeck, Darius; Falk, Erlin; Feldman, Marc D.; Fitzgerald, Peter; Garcia, Hector; Gonzalo, Nieves; Granada, Juan F.; Guagliumi, Giulio; Holm, Niels R.; Honda, Yasuhiro; Ikeno, Fumiaki; Kawasaki, Masanori; Kochman, Janusz; Koltowski, Lukasz; Kubo, Takashi; Kume, Teruyoshi; Kyono, Hiroyuki; Lam, Cheung Chi Simon; Lamouche, Guy; Lee, David P.; Leon, Martin B.; Maehara, Akiko; Manfrini, Olivia; Mintz, Gary S.; Mizuno, Kyiouchi; Morel, Marie-Angéle; Nadkarni, Seemantini; Okura, Hiroyuki; Otake, Hiromasa; Pietrasik, Arkadiusz; Prati, Francesco; Räber, Lorenz; Radu, Maria D.; Rieber, Johannes; Riga, Maria; Rollins, Andrew; Rosenberg, Mireille; Sirbu, Vasile; Serruys, Patrick W. J. C.; Shimada, Kenei; Shinke, Toshiro; Shite, Junya; Siegel, Eliot; Sonada, Shinjo; Suter, Melissa; Takarada, Shigeho; Tanaka, Atsushi; Terashima, Mitsuyasu; Troels, Thim; Uemura,

This publication could be one of several versions: author's original, accepted manuscript or the publisher's version. / La version de cette publication peut être l'une des suivantes : la version prépublication de l'auteur, la version acceptée du manuscrit ou la version de l'éditeur.

For the publisher's version, please access the DOI link below. / Pour consulter la version de l'éditeur, utilisez le lien DOI ci-dessous.

Publisher's version / Version de l'éditeur:

<https://doi.org/10.1016/j.jacc.2011.09.079>

Journal of the American College of Cardiology, 59, 12, pp. 1058-1072, 2012-03-12

NRC Publications Archive Record / Notice des Archives des publications du CNRC :

<https://nrc-publications.canada.ca/eng/view/object/?id=94d6cee4-64c0-43c6-bd5c-f855360eca0f>

<https://publications-cnrc.canada.ca/fra/voir/objet/?id=94d6cee4-64c0-43c6-bd5c-f855360eca0f>

Access and use of this website and the material on it are subject to the Terms and Conditions set forth at

<https://nrc-publications.canada.ca/eng/copyright>

READ THESE TERMS AND CONDITIONS CAREFULLY BEFORE USING THIS WEBSITE.

L'accès à ce site Web et l'utilisation de son contenu sont assujettis aux conditions présentées dans le site

<https://publications-cnrc.canada.ca/fra/droits>

LISEZ CES CONDITIONS ATTENTIVEMENT AVANT D'UTILISER CE SITE WEB.

Questions? Contact the NRC Publications Archive team at

PublicationsArchive-ArchivesPublications@nrc-cnrc.gc.ca. If you wish to email the authors directly, please see the first page of the publication for their contact information.

Vous avez des questions? Nous pouvons vous aider. Pour communiquer directement avec un auteur, consultez la première page de la revue dans laquelle son article a été publié afin de trouver ses coordonnées. Si vous n'arrivez pas à les repérer, communiquez avec nous à PublicationsArchive-ArchivesPublications@nrc-cnrc.gc.ca.

Consensus Standards for Acquisition, Measurement, and Reporting of Intravascular Optical Coherence Tomography Studies

A Report From the International Working Group for Intravascular Optical Coherence Tomography Standardization and Validation

Guillermo J. Tearney, MD, PhD, *Writing Committee Co-Chair*,*
 Evelyn Regar, MD, PhD, *Writing Committee Co-Chair*,† Takashi Akasaka, MD, *Writing Committee Co-Chair*,‡
 Tom Adriaenssens, MD, Peter Barlis, MD, Hiram G. Bezerra, MD, Brett Bouma, PhD,
 Nico Bruining, PhD, Jin-man Cho, MD, PhD, Saqib Chowdhary, PhD, Marco A. Costa, MD, PhD,
 Ranil de Silva, MD, PhD, Jouke Dijkstra, PhD, Carlo Di Mario, MD, PhD, Darius Dudeck, MD, PhD,
 Erlin Falk, MD, PhD, Marc D. Feldman, MD, Peter Fitzgerald, MD, Hector Garcia, MD,
 Nieves Gonzalo, MD, Juan F. Granada, MD, Giulio Guagliumi, MD, Niels R. Holm, MD,
 Yasuhiro Honda, MD, Fumiaki Ikeno, MD, Masanori Kawasaki, MD, Janusz Kochman, MD, PhD,
 Lukasz Koltowski, MD, Takashi Kubo, MD, PhD, Teruyoshi Kume, MD, Hiroyuki Kyono, MD,
 Cheung Chi Simon Lam, MD, Guy Lamouche, PhD, David P. Lee, MD, Martin B. Leon, MD,
 Akiko Maehara, MD, Olivia Manfrini, MD, Gary S. Mintz, MD, Kyiouchi Mizuno, MD,
 Marie-angéle Morel, MD, Seemantini Nadkarni, PhD, Hiroyuki Okura, MD, Hiromasa Otake, MD,
 Arkadiusz Pietrasik, MD, Francesco Prati, MD, Lorenz Räber, MD, Maria D. Radu, MD,
 Johannes Rieber, MD, Maria Riga, MD, Andrew Rollins, PhD, Mireille Rosenberg, PhD, Vasile Sirbu, MD,
 Patrick W. J. C. Serruys, MD, PhD, Kenei Shimada, MD, Toshiro Shinke, MD, Junya Shite, MD,
 Eliot Siegel, MD, Shinjo Sonada, MD, Melissa Suter, PhD, Shigeho Takarada, MD, PhD,
 Atsushi Tanaka, MD, PhD, Mitsuyasu Terashima, MD, Thim Troels, MD, PhD, Shiro Uemura, MD, PhD,
 Giovanni J. Ughi, PhD, Heleen M.M. van Beusekom, PhD, Antonius F.W. van der Steen, PhD,
 Gerrit-Ann van Es, PhD, Gijs van Soest, PhD, Renu Virmani, MD, Sergio Waxman, MD,
 Neil J. Weissman, MD, Giora Weisz, MD

Boston, Massachusetts; Rotterdam, the Netherlands; and Wakayama, Japan

Objectives

The purpose of this document is to make the output of the International Working Group for Intravascular Optical Coherence Tomography (IWG-IVOCT) Standardization and Validation available to medical and scientific communities, through a peer-reviewed publication, in the interest of improving the diagnosis and treatment of patients with atherosclerosis, including coronary artery disease.

Background

Intravascular optical coherence tomography (IVOCT) is a catheter-based modality that acquires images at a resolution of ~10 μm, enabling visualization of blood vessel wall microstructure in vivo at an unprecedented level of detail. IVOCT devices are now commercially available worldwide, there is an active user base, and the interest in using this technology is growing. Incorporation of IVOCT in research and daily clinical practice can be facilitated by the development of uniform terminology and consensus-based standards on use of the technology, interpretation of the images, and reporting of IVOCT results.

Methods

The IWG-IVOCT, comprising more than 260 academic and industry members from Asia, Europe, and the United States, formed in 2008 and convened on the topic of IVOCT standardization through a series of 9 national and international meetings.

Results

Knowledge and recommendations from this group on key areas within the IVOCT field were assembled to generate this consensus document, authored by the Writing Committee, composed of academicians who have participated in meetings and/or writing of the text.

Conclusions

This document may be broadly used as a standard reference regarding the current state of the IVOCT imaging modality, intended for researchers and clinicians who use IVOCT and analyze IVOCT data. (J Am Coll Cardiol 2012;59:1058–72) © 2012 by the American College of Cardiology Foundation

This is an open access article under the [CC BY-NC-ND](#)

Introduction

International Working Group for Intravascular OCT Standardization and Validation

This document is the output of the International Working Group for Intravascular OCT Standardization and Validation (IWG-IVOCT). The Working Group consists of experts in intravascular optical coherence tomography (IVOCT) from Asia, Europe, and the United States. The academic and industry sectors are represented. Today, there are a total of 260 members in the IWG-IVOCT: 60% from academia and 40% from industry, including representation from all current IVOCT manufacturers. The academic membership is approximately equally split between the United States, European Union, and Asia, with additional members from Australia and South America.

See page 1090

IWG-IVOCT was initiated at a meeting held in Prague, Czech Republic, on September 25, 2008, where the international intravascular OCT community expressed the need for a consensus document. A decision was made to go forward with a series of meetings to attain consensus on the use of IVOCT technology and interpretation of IVOCT images. As of the date of this publication, a total of 9 IWG-IVOCT meetings have been conducted (Prague [n = 1], San Francisco [n = 3], Barcelona [n = 1], London [n = 1], Kobe [n = 1], Paris [n = 1] and Washington, DC [n = 1]).

This document was written by the Writing Committee, comprised of academicians who have participated in meetings and/or the writing of the document. Industry members were active participants in IWG-IVOCT, but did not participate on the Writing Committee. The American

College of Cardiology Task Force on Clinical Expert Consensus Documents did not commission this work.

Purpose of This Document

IVOCT is an emerging imaging technology for evaluating the cross-sectional and 3-dimensional (3D) microstructure of blood vessels at a resolution of approximately 10 μm . Because of its higher resolution than intravascular ultrasound (IVUS), IVOCT may be capable of characterizing the superficial structure of the vessel wall in greater detail. As a result, it is believed that IVOCT may become an important imaging technique for medical fields that involve pathological assessment of blood vasculature, including cardiology. In order to facilitate uniform use and adoption of this technology, the IWG-IVOCT has worked collaboratively to generate standard nomenclature, usage guidelines, image interpretation criteria, measurement methodology, and reporting of IVOCT results. This consensus document is the output of this effort, intended for researchers and clinicians who use IVOCT and analyze IVOCT data. Because the vast majority of knowledge about IVOCT pertains to the coronary arteries, this document focuses on coronary application of IVOCT. This document will be considered current until subsequently revised by IWG-IVOCT.

Methodology

Different IWG-IVOCT subgroups were formed to address the main topic areas within the IVOCT field. Each subgroup was tasked with summarizing: 1) what is known to date; 2) common pitfalls or roadblocks; and 3) what is not known to date within their respective topic area. In addition, the subgroups were asked to provide recommendations or guidelines regarding what are currently thought to be acceptable approaches for each topic. Information was obtained from each of the subgroups and assembled by the IWG-IVOCT organizers to provide a draft consensus document, which was then circulated to the Writing Committee for review and editing. Comments were also solicited from the entire IWG-IVOCT during the internal review process.

The format of this document is patterned closely after the American College of Cardiology Clinical Expert Consensus Document on Standards for Acquisition, Measurement, and Reporting of Intravascular Ultrasound Studies by Mintz *et al.* (1), hereinafter termed *JACC IVUS Consensus Document*. Because of the similarities between IVUS and

From *The Massachusetts General Hospital and the Wellman Center for Photomedicine, Boston, Massachusetts; †Erasmus Medical Center, Rotterdam, the Netherlands; and the ‡Wakayama Medical School, Wakayama, Japan. Drs. Tearney, Regar, and Akasaka are co-chairs of the International Working Group for Intravascular OCT Standardization and Validation (IWG-IVOCT) and co-chairs of the Writing Committee for this document. The IWG-IVOCT effort has been partially sponsored by gifts and educational grants from Merck, Boston Scientific, and the Center for Integration of Medicine & Innovative Technology. Dr. Akasaka is on the clinical advisory board of St. Jude Medical and Terumo Inc.; and has received research funding from Abbott Vascular Japan, St. Jude Medical Japan, Goodman Inc., and Boston Scientific Inc. All members of the Writing Committee, as well as their affiliations and relationships with industry, are listed in the Online Supplementary Material.

Manuscript received February 28, 2011; revised manuscript received August 9, 2011, accepted September 27, 2011.

Abbreviations and Acronyms

- CSA** = cross-sectional area
- DICOM** = Digital Imaging and Communication in Medicine
- EEM** = external elastic membrane
- FD-OCT** = frequency-domain optical coherence tomography
- IEM** = internal elastic membrane
- IVOCT** = intravascular optical coherence tomography
- IVUS** = intravascular ultrasound
- IWG-IVOC** = International Working Group on Intravascular Optical Coherence Tomography Standardization and Validation
- NIR** = near-infrared
- OCT** = optical coherence tomography
- TCFA** = thin-capped fibroatheroma
- TD-OCT** = time-domain optical coherence tomography

IVOCT, whenever possible, terminology and methods that exist for IVUS have been adopted for IVOCT. For pathological descriptions, the nomenclature and classification scheme follows that of Virmani et al. (2), when applicable.

For this document, the quality of evidence supporting the findings of the image interpretation IWG-IVOC subgroup is as follows:

Evidence level: High. Homogeneous evidence from multiple, well-designed, cohort (descriptive) trials, each involving a number of samples to be of sufficient statistical power or multiple histopathologic correlative studies of sufficient statistical power.

Evidence level: Medium. From at least 1 well-designed trial, involving a number of samples to be of sufficient statistical power or a single histopathologic correlative study of sufficient statistical power.

Evidence level: Low. Evidence based on clinical experience, descriptive studies, or reports of expert committees or histopathologic correlative case studies.

logic correlative case studies.

Levels of Evidence Bibliography

A bibliography listing of representative papers that support image interpretation levels of evidence is provided in the Online Supplementary Material (Online Table 1).

Physical Principles of OCT Imaging

OCT is a light-based imaging modality that generates high-resolution cross-sectional images of tissue microstructure (3). The underlying concept of OCT is analogous to that of ultrasound; by measuring the delay time of optical echoes reflected or backscattered from subsurface structures in biological tissues, structural information as a function of depth within the tissue can be obtained.

IVOC light is in the *near infrared* (NIR) range, typically with wavelengths of approximately 1.3 μm, which are not visible to the human eye. OCT measures the time delay of the light that is reflected or backscattered from tissue, and that is collected by the catheter, by using a technique known as *interferometry*. Light from the OCT system is split so that a portion of it travels to the patient (*sample arm*) through a catheter and another portion travels a predetermined distance (*reference arm*). After being reflected from tissue and

collected by the catheter, the sample arm light is combined with the reference arm light and detected by a *detector*. When the distance that the sample and reference arm lights have traveled are roughly equivalent, a pattern of high and low intensities are detected, known as interference. This interference pattern is analyzed by the OCT system to determine the amount of backscattering as a function of delay time or depth within the tissue (A-line). A cross-sectional IVOCT image is obtained by recording A-lines as the beam is scanned across the sample by rotating the optics in the catheter. The axial range over which an OCT image can be obtained is termed the *ranging depth*. This parameter typically ranges from 4 to 6 mm. For circular images in IVOCT, the total width of the image is twice this value, or 8 to 12 mm in diameter.

There are 2 types of IVOCT systems: earlier time-domain OCT (TD-OCT) and more recent Fourier-domain OCT systems, also known as frequency domain OCT (FD-OCT), swept-source OCT, or optical frequency domain imaging (OFDI). The main difference between TD-OCT and FD-OCT systems is that FD-OCT systems are capable of obtaining A-lines at much higher imaging speeds, facilitating rapid, 3D pullback imaging during the administration of a nonocclusive flush of an optically transparent media such as Lactated Ringer's or radiocontrast.

Like IVUS, IVOCT image quality is in part dependent on spatial resolution. Spatial resolution, or the minimum distance between closely spaced objects that can be independently detected by the imaging system, has 2 directions: axial (parallel to the light beam) and *lateral or transverse* (perpendicular to the light beam). The *axial resolution* for OCT is dependent on the spectral bandwidth, or range of wavelengths in the light source, and is typically approximately 10 μm. Near the tip of the catheter, light is focused by a small lens and directed toward the vessel wall. The light converges to a minimum diameter spot (focus) outside the catheter and then diverges. The focal location is typically 1 to 3 mm outside the catheter's sheath. The lateral resolution of the OCT image is best at the focus, where the diameter, *d*, of the spot is at a minimum, *d*₀, typically between 20 and 40 μm. The depth of focus is twice the Rayleigh range ±*z*_r = π(*d*/2)²/λ, defined as the axial distance away from the focus where the spot diameter increases by √2. The diameter of the beam a given axial distance, *z*, from the focal location is given by:

$$d = d_0 \sqrt{1 + \left(\frac{z}{z_r}\right)^2}$$

The *spot size*, and therefore the lateral resolution and the image quality, are poorer in the portions of the image that are distant from the focal location. Moreover, objects that are distant from the focus may appear larger than expected. In addition to the spot diameter, the number of A-lines in the image can also affect lateral resolution

along the *circumferential or rotational dimension*. If there are not enough *A-lines* acquired per focused spot, then small or closely spaced objects may not be able to be resolved in the OCT image. The focus also affects the intensity of the OCT image, which has a stronger OCT intensity at the *focus* and weaker OCT intensity away from the focus.

Refractive index is a property of a material that governs the speed of light through the material. Because the speed of light is slower in flushing media and tissue than it is in air, the distances in the images need to be corrected for this delay. IVOCT manufacturers provide a correction for refractive index by dividing the distance in the axial direction in the IVOCT image by the estimated refractive index of the flushing media and tissue. Once corrected, the images may be used to obtain area and length measurements. The more precisely the refractive indices are known, the more accurate the measurements. Future research to determine the refractive index of different transparent media, flushing media, and various tissue types will improve measurement accuracies.

As a light beam encounters a boundary between 2 tissues with different refractive indices (optical impedances), a portion of the light is scattered, and a portion is transmitted. IVOCT measures light that is reflected or backscattered from the interface and is collected by the catheter. The amount of *backscattered light*, and therefore the intensity of the OCT image, is dependent on the magnitude of the difference in refractive indices of the tissues. For larger planar structures with dimensions that are large compared with the wavelength of light, such as stent struts, the *reflected light* is higher when the object is perpendicular to the direction of the optical beam.

Contrast affects the quality of the image and is related to the difference in backscattered intensities that distinguish an object from other objects and the background. *Dynamic range* is the difference between the minimal and maximal reflected signals that can be detected or visualized by the OCT system. The typical dynamic range of OCT systems ranges from 30 to 50 dB (10^3 to 10^5). OCT instruments are often characterized by *sensitivity*, which is a parameter describing how faint a backscattered signal can be detected, and is typically in the range of -90 to -110 dB (10^{-9} to 10^{-11}).

Penetration depth is a term that defines how deeply within tissue one can obtain OCT image data that are higher background noise. As the light passes through the tissue, it is attenuated by scattering and *absorption*. The predominant form of *attenuation* encountered by IVOCT systems that have wavelengths near 1.3 μm is scattering. Highly attenuating tissue, such as lipid, has a low penetration depth, and therefore, IVOCT does not see as deeply within some lipid-containing plaques. Other tissues, such as collagen and calcium, have lower attenuation, and as a result, IVOCT can see deeper into these tissues (Online Table 2). For this reason, the penetration depth in arteries depends on tissue

type and usually ranges from 0.1 to 2.0 mm using typical IVOCT NIR light. IVOCT cannot image through blood because blood attenuates the IVOCT light before it reaches the artery wall. As a result, IVOCT images are acquired as blood is flushed from the field of view.

Equipment for IVOCT Imaging

IVOCT consoles, catheters, and Digital Imaging and Communication in Medicine (DICOM) supplement 151 are described in the Online Supplementary Material.

IVOCT Artifacts

Recognition of artifacts is critical for proper interpretation of IVOCT images. A complete listing of the artifacts seen in IVOCT images, as identified by IWG-IVOCT, is described (including Online Figs. 2 to 11) in the Online Supplementary Material.

IVOCT Image Display Techniques

There are various ways to display the IVOCT image data, and these display techniques may affect image interpretation. Descriptions of IVOCT image display methods are presented in the Online Supplementary Material.

Image Acquisition Protocols

Concomitant medication, patient, and lesion selection

Like IVUS, current practice requires that the patients be anticoagulated, typically with heparin, before inserting the guidewire into the coronary artery. If it is not contraindicated, image acquisition should be conducted after the administration of intracoronary nitroglycerin to minimize the potential for catheter-induced vasospasm.

For patients who have severely impaired left ventricular function or those presenting with significant hemodynamic compromise, IVOCT should be performed with caution, because IVOCT is conducted while clearing blood from the field of view by flushing the artery with crystalloid/radiocontrast media. Furthermore, IVOCT should be used with caution in patients with a single remaining vessel or those with markedly impaired renal function or known allergy to the flushing media.

In lesions with coexisting rich collateral blood flow or cases in which coaxial positioning of the guiding catheter into the coronary ostium is not feasible, and as a consequence blood clearance is insufficient, wire-type IVOCT combined with a proximal occlusion balloon may be useful to obtain clear IVOCT imaging.

In lesions with near complete stenosis or total occlusion of an artery, it is recommended that, if clinically indicated, the antegrade blood flow be restored before IVOCT examination of that artery in order to allow the flushing media to adequately clear blood from the artery.

Because the profile of the guide wire catheter, ImageWire (available for TD-OCT only at the time of writing this document), is smaller than that of drive cable type catheters typically used for FD-OCT (0.014-inch or ~1.1-F vs. 2.4-F to 3.2-F), clinical application of these devices may be different. The imaging procedure for FD-OCT is more likely to be straightforward than for TD-OCT (see the following text). However, for vessels with severe stenosis, FD-OCT catheters with larger profiles are sometimes difficult or unable to pass through severely narrowed lesions (i.e., calcified or diffusely obstructed lesions).

Image Acquisition Techniques

As with IVUS, IVOCT interrogation can be conducted via a manual or via motorized pullback (1). Because NIR light is unable to penetrate through blood, the field of view must be cleared from blood during image acquisition. Several techniques have been developed to clear blood from the artery in order to obtain high-quality images of the artery wall. Because the imaging and pullback speeds of FD-OCT systems are much higher than those of TD-OCT systems, approaches for clearing blood from the artery may differ for the 2 systems. In this section, we describe widely used image acquisition techniques for each type of IVOCT system.

TD-OCT image acquisition techniques. There are 2 approaches for TD-OCT image acquisition: the occlusive technique and the nonocclusive technique. Both of these TD-OCT image acquisition methods remove blood from the artery using a transparent media flush and use helical pullback imaging, but the occlusive technique mandates the inflation of a balloon proximal to the imaging site. To date, most TD-OCT has been performed using the occlusive technique, but improvements in the acquisition speeds of TD-OCT systems have allowed nonocclusive flushing to be used as an alternative image acquisition method. The nonocclusive flushing technique is also applied in cases in which the occlusion balloon cannot be effectively deployed to limit native coronary flow, such as for ostial coronary lesions. Nonocclusive flushing may cause less myocardial ischemia than the proximal balloon occlusion approach and avoids a potential risk of vessel injury by proximal balloon occlusion. Both TD-OCT image acquisition methods are detailed in the Online Supplementary Material.

FD-OCT image acquisition techniques. Because of its higher imaging speed, helical pullback image acquisition with FD-OCT is primarily conducted with nonocclusive flushing techniques for removing blood from the artery. A detailed description of FD-OCT image acquisition protocols is presented in the Online Supplementary Material.

Safety Data

TD-OCT. In a multicenter registry including 468 patients imaged with the occlusive flush or nonocclusive flush technique, the most frequent events were transient chest pain and electrocardiogram changes (QRS widening/ST-segment depression/elevation), observed in 47.6% and

45.5% of cases, respectively. Major complications included 5 cases (1.1%) of ventricular fibrillation due to balloon occlusion and/or deep guide catheter intubation, 3 cases (0.6%) of air embolism, and 1 case (0.2%) of vessel dissection. There were no cases of coronary spasm or major adverse coronary events during or within the 24-hour period after TD-OCT examination (4).

FD-OCT. One clinical paper reported no serious electrocardiogram changes or complications with FD-OCT imaging using the nonocclusive flush technique (5). In preliminary registries of patients imaged with FD-OCT, the most frequent events were transient T-wave inversion or ST-segment depression, observed in 10% of cases (6). No major complications during or within the 24-h period after FD-OCT examination were observed (6).

Qualitative Assessment

Definition of Lesion and Reference Segment

The definitions of *Lesion* and *Reference Segment* from JACC IVUS Consensus Document have been adopted for IVOCT. These definitions are presented with modifications next:

Proximal reference. The site with the largest lumen proximal to a stenosis but within the same segment (usually within 10 mm of the stenosis, with no major intervening branches). This may not be the site with the least plaque.

Distal reference. The site with the largest lumen distal to a stenosis but within the same segment (usually within 10 mm of the stenosis, with no intervening branches). This may not be the site with the least plaque.

Largest reference. The largest of either the proximal or distal reference sites.

Average reference lumen size: the average value of lumen size at the proximal and distal reference sites.

Lesion. A lesion is seen by IVOCT as a mass lesion within the artery wall, focal intimal thickening, or loss of the layered intima, media, adventitia architecture.

Stenosis. A stenosis is a lesion that compromises the lumen by at least 50% by cross-sectional area (CSA), as compared with a predefined reference segment lumen.

Worst stenosis (T-1). The stenosis with the smallest lumen size.

Secondary stenoses (T-2, T-3, and so on). Lesions meeting the definition of a stenosis, but with lumen sizes larger than the worst stenosis.

Blood

Because blood attenuates light and can affect the quality of the IVOCT image, it should be recognized in the images. Blood has high superficial backscattering and has high attenuation below the surface (Evidence Level: High). When mixed with optically transparent flushing media, it may form many different patterns within the artery lumen (Online Fig. 8). Blood can be confused with red thrombus.

Care should be taken when interpreting plaque components through blood, as blood can *shadow* the IVOCT signal.

Lesion Morphology

Like IVUS, IVOCT images are fundamentally different from histology. However, owing to the higher, 10- μm resolution of IVOCT, images obtained using IVOCT share some similarities with histological images. The capability of IVOCT to detect and quantify specific contents that are analogous to histological features may therefore be possible in some circumstances. As a result, pathological descriptors have been used in this document, with the classification and nomenclature following that of Virmani *et al.* (2). We note that not all features capable of being identified by histology have been verified to also be seen by IVOCT, so caution must be taken when applying histological descriptors to IVOCT images. The extent to which IVOCT can describe pathology has yet to be determined.

Consensus was achieved as follows on qualitative image interpretation pertaining to single cross-sectional image diagnosis. Because most implementations of IVOCT obtain multiple sequential images during pullback, seeing a feature in more than 1 frame improves diagnostic confidence.

Normal vessel wall or intimal thickening. The normal vessel wall is characterized by a layered architecture, comprising a highly backscattering or signal-rich intima (thin), a media that frequently has low backscattering or is signal-

poor, and a heterogeneous and frequently highly backscattering adventitia (Evidence Level: High) (Fig. 1). The periadventitial tissues may contain IVOCT data consistent with adipocytes, characterized by large clear structures resembling cells and/or vessels. With IVOCT, the internal elastic membrane (IEM) is defined as the border between the intima and media, and the external elastic membrane (EEM) is defined as the border between the media and the adventitia. On occasion, these interfaces may be visualized as highly backscattering thin structures bordering the intima-media (green arrow) or media-adventitia (yellow arrow) interfaces, respectively (Fig. 1, inset).

Atherosclerotic plaque or atheroma. An atherosclerotic plaque is defined as a mass lesion (focal thickening) or loss of a layered structure of the vessel wall (Evidence Level: High). For some plaques, the adventitia, EEM, deep edge of the intima, and/or IEM may be identified (Fig. 2A), whereas for others, these features may not be seen due to the attenuation of light as it is transmitted through plaque tissues (Fig. 2B).

Fibrous plaque. A fibrous plaque (Figs. 2A and 2B) has high backscattering and a relatively homogeneous IVOCT signal (Evidence Level: High). Sometimes the IEM or EEM may be identified in fibrous plaques (Fig. 2A). Caution should be exercised when characterizing a lesion as fibrous plaque if the IEM or EEM cannot be identified. Sometimes, the limited penetration depth of IVOCT does not allow the accurate detection of deep signal-poor areas possibly representing necrotic core or calcium behind fibrous tissue. Fibrous plaques by IVOCT may be composed of collagen or smooth muscle cells. Although it has been postulated that proteoglycans and type III collagen have a lower OCT signal intensity, the relationship between the OCT signal and type III collagen and proteoglycans has not yet been established.

Fibrocalcific plaque. A fibrocalcific plaque contains IVOCT evidence of fibrous tissue (defined previously), along with calcium that appears as a signal-poor or heterogeneous region with a sharply delineated border (leading, trailing, and/or lateral edges) (Evidence Level: High) (Figs. 2C and 2D). This definition applies for larger calcifications; the IVOCT appearance of small calcifications, including microcalcifications, has not been established.

Necrotic core. A necrotic core by IVOCT is a signal-poor region within an atherosclerotic plaque, with poorly delineated borders, a fast IVOCT signal drop-off, and little or no OCT signal backscattering, within a lesion that is covered by a fibrous cap (Evidence Level: Low) (Fig. 3). The necrotic core may also contain IVOCT evidence of cholesterol crystals. It is important to note the distinction between signal-poor regions of calcium, which have sharply delineated borders, as opposed to signal-poor regions of necrotic core, which have poorly defined or diffuse borders. Caution must be exercised when diagnosing necrotic core deep in the tissue, as the attenuation of the IVOCT signal may present as a signal-poor region. As such, IVOCT may be more accurate for identifying necrotic cores that are close to the

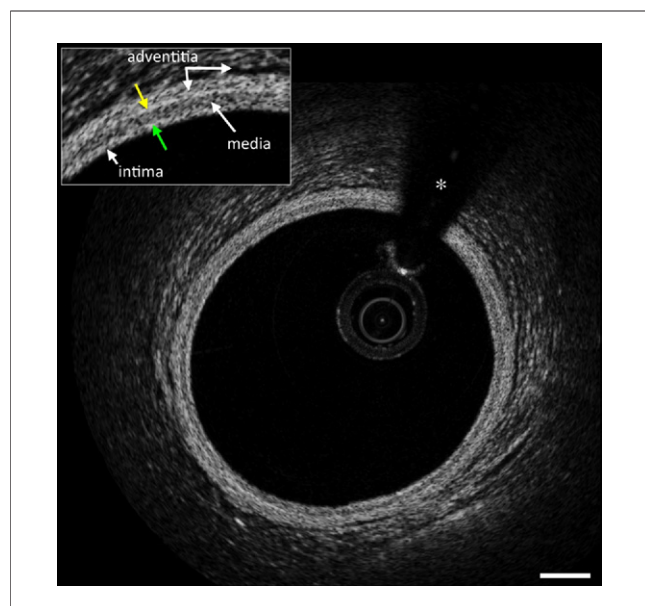


Figure 1 Normal Artery Wall

Normal artery wall shows a 3-layered architecture, comprising a high backscattering, thin intima, a low backscattering media, a heterogeneous and/or high backscattering adventitia, IEM (green arrow), and EEM (yellow arrow) (inset, $\times 2$). Scale bars represent 500 μm . EEM = external elastic membrane; IEM = internal elastic membrane; IVOCT = intravascular optical coherence tomography. *Guide-wire artifact. IVOCT technology, image contributor and institution, and commercial IVOCT vendor for each figure is provided in the Online Supplementary Material.

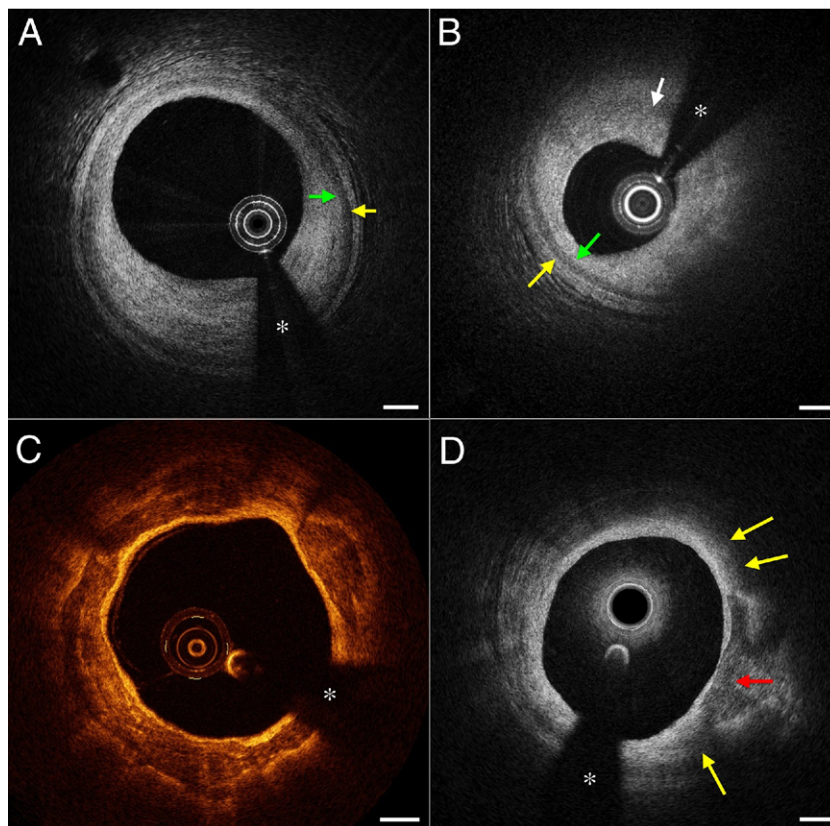


Figure 2 Fibrous and Fibrocalcific Plaques

(A) Fibrous plaque with IEM (green arrow) and EEM (yellow arrow). (B) Plaque without IEM or EEM (white arrow). The EEM (yellow arrow) and IEM (green arrow) can be visualized opposite to the main lesion. (C) Fibrocalcific plaque showing circumferential signal-poor heterogeneous region with well-delineated borders. (D) Mixed plaque with focal calcific deposit comprising regions with sharply delineated borders, consistent with calcium (red arrow), and adjacent signal-poor areas with poorly delineated borders, suggestive of lipid (yellow arrows). Scale bars represent 500 μm . IVOCT technology, image contributor and institution, and commercial IVOCT vendor for each figure is provided in the Online Supplementary Material. *Guide-wire artifact. Abbreviations as in Figure 1.

endoluminal surface. Certain plaque components such as macrophages, which have a high attenuation, may reside at the surface of a plaque and generate the appearance of a signal-poor region below. Artifacts, such as tangential signal dropout (Online Fig. 10), blood, or red thrombus, may also create the appearance of a necrotic core, when one is not actually present. It is recommended that studies be performed *ex vivo* to correlate IVOCT findings with histopathologic determination of necrotic core that is devoid of collagen matrix. Because light does not penetrate well through the necrotic core, it was generally agreed that IVOCT is not capable of measuring the thickness, area, or volume of necrotic cores when the EEM cannot be identified.

IVOCT histopathologic correlative studies have been conducted, showing a good correspondence between signal-poor IVOCT regions with poorly defined or diffuse borders and a broader histopathologic category known as “lipid pool” (Evidence Level: High). In these studies, a lipid pool corresponds histologically to either a necrotic core or a region within pathological intimal thickening that contains extracellular lipid or proteoglycans. At present, there are no definitive published

studies directly comparing IVOCT lipid pool-containing plaques with necrotic core by histology, and as a result, the Evidence Level was determined to be Low for IVOCT delineation of necrotic core. Nevertheless, there are multiple studies demonstrating that these lesions are more commonly found at the culprit site in patients with acute coronary syndrome and acute myocardial infarction, compared with patients with stable angina.

Fibrous cap. A fibrous cap is a tissue layer, which is often signal-rich, overlying a signal-poor region (Evidence Level: High) (Fig. 3). Whether or not the cap is signal-rich or signal-poor and the implications of IVOCT intensity gray-scale values of the cap remains an open question.

Fibroatheroma. As follows from the preceding descriptions, a fibroatheroma is a lesion with an IVOCT-delineated fibrous cap and a necrotic core (Evidence Level: Low).

OCT thin-capped fibroatheroma. An OCT thin-capped fibroatheroma (OCT-TCFA) is defined as an IVOCT-delineated necrotic core with an overlying fibrous cap where the minimum thickness of the fibrous cap is less than a predetermined threshold (Figs. 3C and 3D) (Evidence

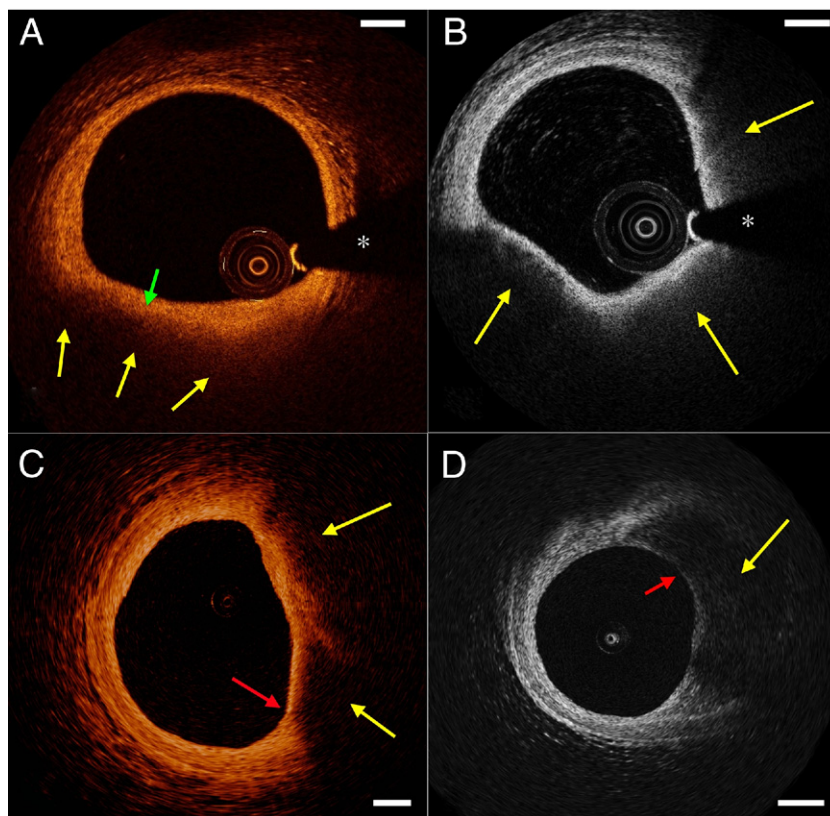


Figure 3 Fibroatheroma

(A) Low IVOCT signal (yellow arrows) with poorly delineated borders and a cap (green arrow) characterize this fibroatheroma. (B) Signal-poor and poorly delineated regions can be seen in more than 3 quadrants circumferentially (yellow arrows). (C) OCT thin-capped fibroatheroma (TCFA) lesion that shows regions with low backscattering (yellow arrows) and a thin fibrous cap (red arrow). (D) OCT-TCFA that shows low backscattering (yellow arrow) covered by a thin fibrous cap (red arrow). Scale bars represent 500 μm . IVOCT technology, image contributor and institution, and commercial IVOCT vendor for each figure is provided in the Online Supplementary Material. *Guide-wire artifact. Abbreviations as in Figure 1.

Level: High). Numbers used by some pathologists as a cutoff minimal cap thickness for TCFA include 65 μm (7); however, these cutoffs should be adjusted when applied to IVOCT images, accounting for the 10% to 20% tissue shrinkage that can occur during histopathologic processing. On the basis of clinical experience and supportive clinical studies, the consensus was that the OCT-TCFA was related to the histopathologic definition of a TCFA. Some studies have used an additional parameter that the necrotic core should subtend an arc that is greater than 90° or comprise more than 1 quadrant of an image displayed in *Cartesian coordinates*. The number of quadrants or the arc angle threshold for OCT-TCFA remains an open question. Recommendations were made to conduct future *ex vivo* studies to correlate IVOCT findings with angular extent. Care should be taken when delineating OCT-TCFA due to the susceptibility of interpreting artifacts as necrotic core (Online Supplementary Material).

Macrophage accumulations. Macrophages may be seen by IVOCT as signal-rich, distinct, or confluent punctate regions that exceed the intensity of background *speckle* noise

(Evidence Level: Medium) (Fig. 4). Macrophages should only be evaluated in the context of a fibroatheroma, as no macrophage validation studies have been reported to date on normal vessel wall or intimal hyperplasia. Macrophages may often be seen at the boundary between the bottom of the cap and the top of a necrotic core. Macrophages attenuate the IVOCT light significantly, and as a result, superficial macrophages can shadow underlying tissue, giving it the appearance of a necrotic core. Macrophage accumulations may also be confused on occasion with microcalcifications, cholesterol crystals, or internal or external elastic membrane. Noting the linear appearance of the cholesterol crystals or laminae can minimize some of these misinterpretations. It should be noted that high axial and lateral resolutions are desired for detection of macrophage accumulations. Whether or not IVOCT can identify individual macrophages is not known.

Intimal vasculature. Vessels within the intima can appear as signal-poor voids that are sharply delineated and can usually be followed in multiple contiguous frames (Evidence Level: Low) (Fig. 5A). It is not known whether these vessels

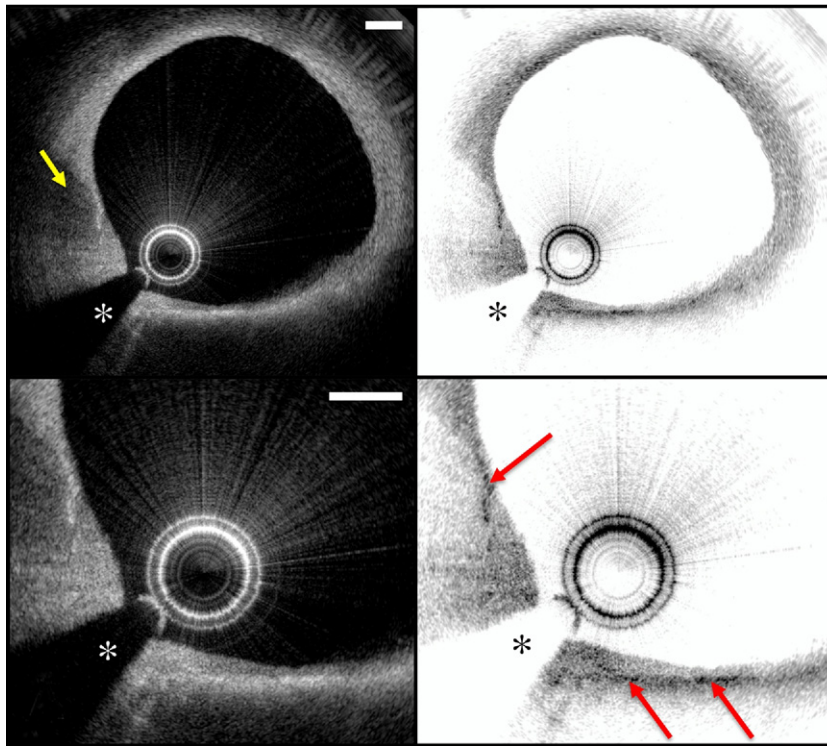


Figure 4 Macrophage Accumulations

Macrophage accumulations appear as confluent or punctate highly backscattering focal regions within the artery wall (**red arrows**), which may be more readily appreciated by visualizing the images using an inverse gray scale look-up table (**right column**). Macrophage accumulations can cause shadowing of underlying tissue structure (**yellow arrow**). **Lower-row panels** are $\times 2$ -magnified versions of **upper-row panels**. Scale bars represent $500\ \mu\text{m}$. IVOCT technology, image contributor and institution, and commercial IVOCT vendor for each figure is provided in the Online Supplementary Material. *Guide-wire artifact. Abbreviations as in Figure 1.

typically communicate with the luminal surface or emanate from the vasa vasorum and whether there is a threshold for the size of these vessels within the intima.

Cholesterol crystals. Cholesterol crystals by IVOCT may appear as thin, linear regions of high intensity, usually associated with a fibrous cap or necrotic core (Evidence Level: Low)

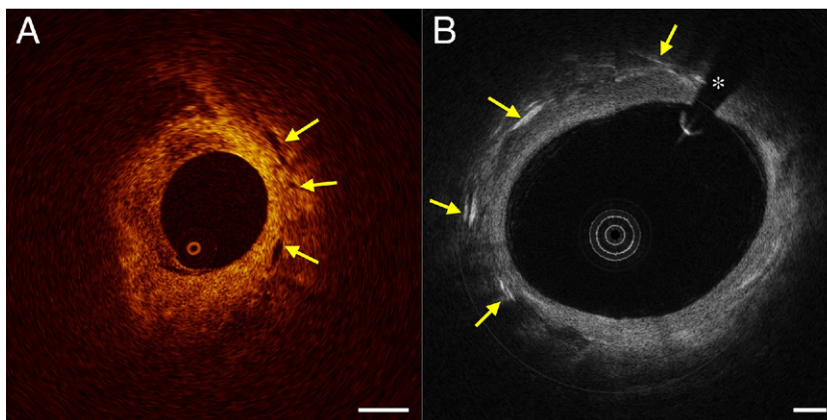


Figure 5 Intimal Vasculature and Cholesterol Crystals

(A) Intimal vessels are well-delineated regions or voids with low IVOCT backscattering (**arrows**). **(B)** Cholesterol crystals appear as linear, highly backscattering structures within the plaque (**arrows**). Scale bars represent $500\ \mu\text{m}$. IVOCT technology, image contributor and institution, and commercial IVOCT vendor for each figure is provided in the Online Supplementary Material. *Guide-wire artifact. Abbreviations as in Figure 1.

(Fig. 5B). For large crystals, 2 reflections (front and back) may sometimes be seen. Although some cholesterol crystals may be seen by IVOCT, sometimes they are not visualized; the reasons for this are not currently understood. The capability of IVOCT to reliably detect cholesterol crystals merits future research.

Thrombus. Thrombus by IVOCT appears as a mass attached to luminal surface or floating within the lumen (Evidence Level: High). When imaging without pullback, some thrombi may be seen to be moving in real-time. IVOCT is capable of discriminating 2 types of thrombus: red (red blood cell-rich) thrombus (Fig. 6A), which is highly backscattering and has a high attenuation (resembles blood), and white (platelet-rich) thrombus (Fig. 6B), which is less backscattering, is homogeneous, and has low attenuation. A small thrombus may be confused with a small dissection or intimal disruption. Thrombus may shadow or obscure underlying structures. Red thrombi may be misinterpreted as necrotic core fibroatheroma. The appearance of organized thrombus by IVOCT is hypothesized to be heterogeneous, but the image characteristics of organized thrombus are not well understood or validated. The capability of IVOCT to identify fibrin as a standalone tissue constituent remains an open question.

Mixed lesions. It is important to note that a single IVOCT cross-sectional or *L-mode image* may contain regions that show IVOCT features that are characteristic of multiple plaque types (e.g., Fig. 2D). These plaques are sometimes also called heterogeneous plaques or mixed lesions.

Dissections and Complications After Intervention

IVOCT definitions of dissections subsequent to intervention largely follow the conventions of the JACC IVUS

Consensus Document and are described in the Online Supplementary Material.

Unstable Lesions and Ruptured Plaque

The TCFA has been associated with plaque rupture and coronary thrombosis at autopsy. No natural history studies have been performed to definitively demonstrate that OCT-TCFAs are associated with future risk for a coronary event. However, these lesions have been found in greater frequency in patients with acute coronary syndrome and acute myocardial infarction, as compared with patients with stable angina. Reports have also shown that these OCT-TCFAs can rupture and thrombose. Macrophages have also been shown to be correlated with symptom severity. Future natural history studies should be conducted to demonstrate the risk of OCT-TCFAs and macrophage-rich plaques for enabling the identification of patients at higher risk for future coronary events.

Ruptured plaques. Ruptured plaques frequently occur in the context of OCT-TCFAs and show features of intimal tearing, disruption, or dissection of the cap (Evidence Level: High) (Fig. 7A). When injected with optically transparent crystalloid or radiocontrast media, these defects may have little or no IVOCT signal and may appear as a cavity.

Plaque ulceration. Plaque ulceration is defined as in JACC IVUS Consensus Document as “A recess in the plaque beginning at the luminal-intimal border” (Evidence Level: Medium).

OCT erosion. Erosions may be composed of IVOCT evidence of thrombus, an irregular luminal surface, and no evidence of cap rupture evaluated in multiple adjacent frames (Evidence Level: Low) (Fig. 7B).

Calcific nodule. A calcific nodule is defined as a single or multiple regions of calcium (defined previously) that pro-

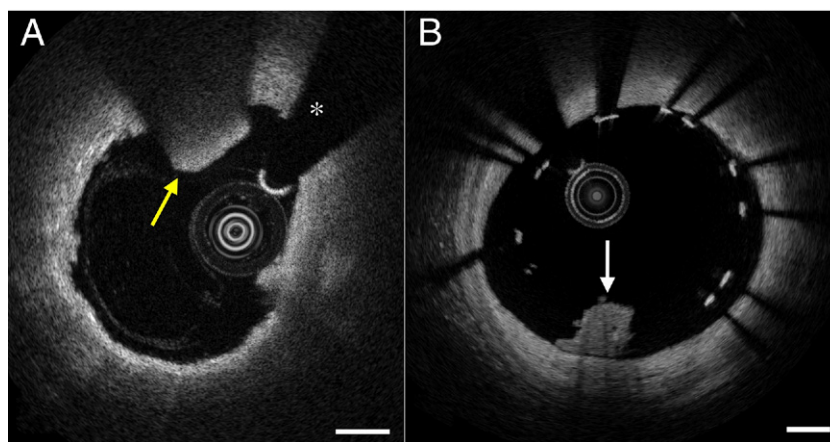


Figure 6 Thrombi

(A) Red thrombus. **Yellow arrow** points to a red thrombus protruding into the lumen with high IVOCT backscattering and attenuation. (B) White thrombus. **White arrow** points to white thrombus with homogeneous backscattering and low attenuation, attached to the surface of coronary artery involving stent struts. There is extensive stent strut malapposition in this image. Scale bars represent 500 μm . IVOCT technology, image contributor and institution, and commercial IVOCT vendor for each figure is provided in the Online Supplementary Material. *Guide-wire artifact. Abbreviations as in Figure 1.

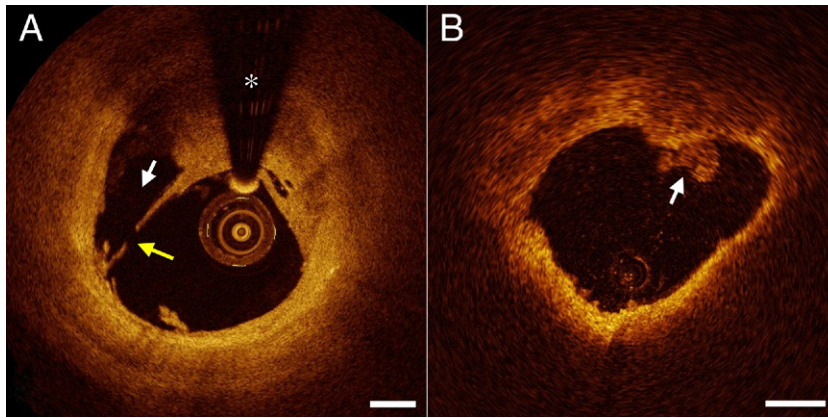


Figure 7 Plaque Rupture and Erosion

(A) Plaque rupture. **Arrow** delineates a broken fibrous cap. The contents of the ruptured plaque are partially washed away by the flush, leaving behind a cavity (**white arrow**). (B) Plaque erosion. A white thrombus (**white arrow**) is present on an irregular luminal surface. There is no evidence of rupture. Scale bars represent 500 μm . IVOCT technology, image contributor and institution, and commercial IVOCT vendor for each figure is provided in the Online Supplementary Material. *Guide-wire artifact. Abbreviations as in Figure 1.

trude into the lumen, frequently forming sharp, jutting angles (Evidence Level: Low).

Thrombus. Thrombus may be identified as white (Figs. 6B and 7A) or red thrombi (Fig. 6A). Thrombi may be sufficiently large to obscure the underlying rupture site or luminal defect.

Unusual Lesion Morphology

IVOCT definitions for true aneurysm, pseudoaneurysm, and true versus false lumen follow the definitions set forth in the JACC IVUS Consensus Document and are presented in the Online Supplementary Material.

Stent Assessment

Because metal stent struts are opaque to light, only the first (leading) surface of individual struts is visualized by IVOCT. The opacity of metal struts also causes a shadow that obscures deeper structures within the vessel wall. The definitions of different parameters of interest for the assessment of stents are as follows:

Prolapse. Prolapse is defined as the projection of tissue into the lumen between stent struts after implantation (Fig. 8A) (Evidence Level: High). Prolapse is more frequently observed when the stent is placed over an OCT-TCFA or necrotic core. It may be difficult to differentiate between prolapse, thrombus, intimal, and intra-stent dissection and neointima.

Apposition. Apposition of the stent struts to the arterial wall can be seen by IVOCT because of its high resolution and capability to identify the tissues surrounding the struts (Evidence Level: High). Malapposition is present when the axial distance between the strut's surface to the luminal surface is greater than the strut thickness (including polymer, if present) (Fig. 8B). If the distance is less than the strut thickness, then the strut is considered apposed. Two forms of apposition have been described in the literature:

protruding, where the endoluminal strut boundary is located above the level of the luminal surface, and embedded, where the endoluminal strut boundary is below the level of the luminal surface; however, the clinical significance of this classification is unclear. It is important to note that before assessing apposition, it is necessary to calibrate the distance and include appropriate corrections for refractive index. Apposition can be described on a per-strut, a per-cross-sectional area, and a per-stent basis.

Thrombus. Thrombus is frequently identified in target lesions and can protrude in-between or over stent struts (Evidence Level: High) (Fig. 6B). The previously described classification scheme for red and white thrombus remains valid.

Dissections. Dissections at the edge of stents are frequently seen by IVOCT (Evidence Level: High) (Figs. 8C and 8D). The classification scheme for dissections is described in the Online Supplementary Material.

OCT strut coverage. The high-resolution capabilities of IVOCT and also its diminished susceptibility to artifacts at the stent strut interface compared with IVUS make it capable of visualizing tissue overlying struts. This capability has been used to evaluate the response to stent implantation. Struts are termed *covered* by IVOCT if tissue can be identified above the struts (Fig. 9A). Struts are dubbed *uncovered* by IVOCT if no evidence of tissue can be visualized above the struts (Fig. 9B, green inset). There are rare observations where struts may have tissue covering only part of the strut; some experts considered the strut to be classified as covered in these cases, whereas others suggested that these struts be classified as having incomplete coverage. At present, IVOCT has not been shown to allow the visualization of endothelium, but this question is still under investigation. In order to not confuse strut coverage by IVOCT with histopathologic determination of endothelial

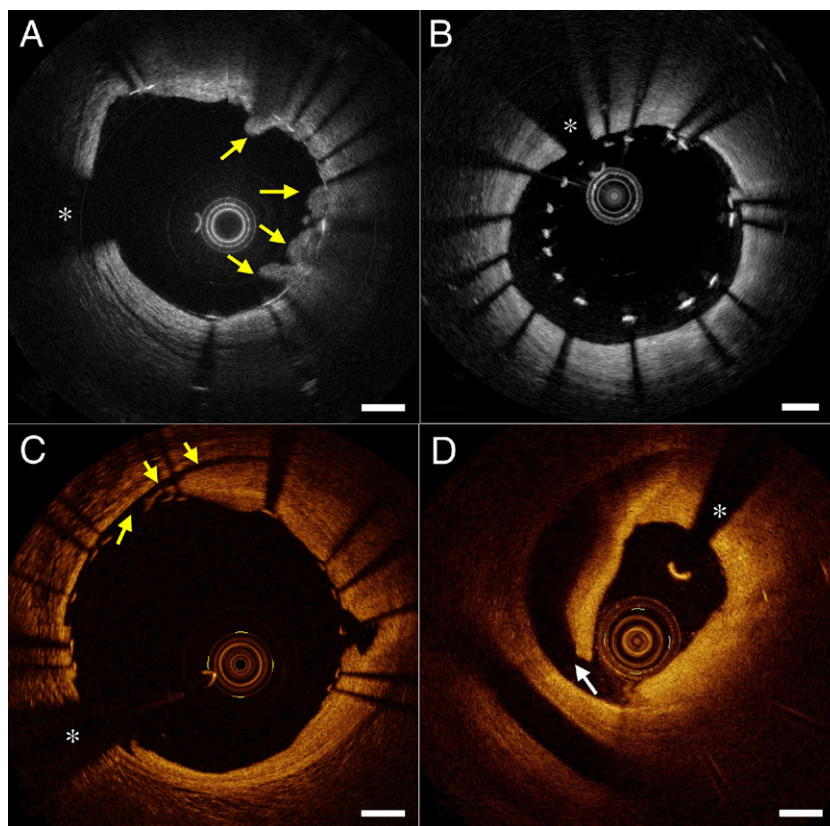


Figure 8 Prolapse, Malapposition, and Dissections

(A) Tissue prolapse. **Arrows** delineate tissue that has prolapsed between stent struts. (B) Stent malapposition showing stent struts that are distant from the luminal surface of the artery wall. (C) A small dissection at edge of stent (**yellow arrows**). (D) A larger dissection (**white arrow**). Scale bars represent 500 μm . IVOCT technology, image contributor and institution, and commercial IVOCT vendor for each figure is provided in the Online Supplementary Material. *Guide-wire artifact. Abbreviations as in Figure 1.

coverage, it is therefore recommended that the term *OCT strut coverage* be used. Additionally, the precise nature of tissue coverage has not been demonstrated, be it fibrin, endothelium, thrombus, neointimal, or other. It has been postulated that IVOCT strut coverage tissue characteristics such as backscattering intensity may provide further discrimination of IVOCT strut coverage tissue type (8); however, it was believed that this topic merited further investigation. In addition, the significance of the intensity of the strut's backscattering has not been established. As with apposition, strut coverage has been reported on a per-strut, per-cross-sectional area basis, or per stent area or volume.

Restenosis. Restenosis by IVOCT may be visualized as signal-poor (Fig. 9C), layered, or signal-rich (Fig. 9D) tissue overlying stent struts. The relationship between the signal intensity of restenosis seen by IVOCT and the underlying tissue composition has only been documented in rare cases and is not generally understood.

Bioabsorbable stents/scaffolds. Depending on the type of material and the progress/process of strut degradation and resorption, the amount of backscattering detected from the struts and the underlying vessel wall will vary. At present,

definitions for resorbable struts have been proposed by Ormiston *et al.* (9) (preserved box, open box, dissolved bright box, and dissolved black box) for one type of bioabsorbable scaffold. It was further noted that the appearances of bioabsorbable struts by IVOCT depends on the scaffold material and the time point of visualization.

Special Considerations

IVOCT serial examinations of atheroma progression/regression, interventional target lesion assessment, and serial examination of stents are described in the Online Supplementary Material.

Quantitative Measurements

Measurements should be made on good-quality images that do not contain artifacts. In order to make accurate measurements, the image should be correctly calibrated for *z*-offset and refractive index. Studies have been published regarding the accuracy of IVOCT measurements and the reproducibility of derived qualitative and quantitative parameters (10–12).

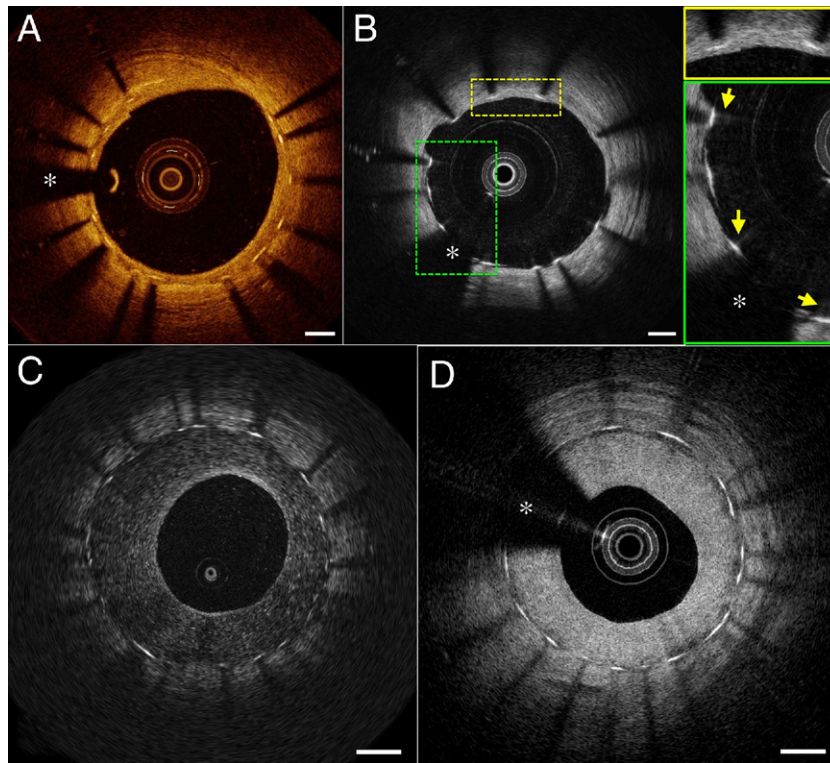


Figure 9 Covered and Uncovered Stent Struts and Restenosis

(A) Covered stent struts. IVOCT signal around and covering stent struts varies. (B) Covered (yellow dotted box) and uncovered (green dotted box) stent struts. Upper inset (yellow, $\times 2$) shows struts with overlying tissue. Lower inset (green, $\times 2$) depicts struts with no apparent overlying tissue coverage. Some of the uncovered struts demonstrate a blooming artifact (yellow arrows, green inset). (C) In-stent restenosis with a low IVOCT signal intensity. (D) In-stent restenosis demonstrating a homogeneous, high-backscattering neointima. Scale bars represent 500 μm . IVOCT technology, image contributor and institution, and commercial IVOCT vendor for each figure is provided in the Online Supplementary Material. *Guide-wire artifact. Abbreviations as in Figure 1.

Border Identification

A description of methodologies used to delineate the borders of the lumen, EEM, and IEM, plaque constituents, and stent and stent struts is provided in the Online Supplementary Material.

In IVUS, it can be difficult to demarcate the IEM and for this reason the EEM is typically used to define the deep boundaries of plaque. In contrast, for IVOCT, either or both the IEM or EEM may be visualized and, therefore, plaque measurements may be computed from either the IEM or EEM when present in the image. Measurements that use the EEM are likely closer to those of IVUS, whereas measurements that use the IEM more closely approximate the pathologic definition of atherosclerosis as a disease of the intima.

Atheroma Measurements

Lumen measurements. Once the lumen has been traced, the lumen measurements performed by IVOCT are similar to that for IVUS and are reproduced for completeness from the JACC IVUS Consensus Document here:

“LUMEN CSA. The area bounded by the luminal border.

MINIMUM LUMEN DIAMETER. The shortest diameter through the *center of mass* of the lumen.

MAXIMUM LUMEN DIAMETER. The longest diameter through the center of mass of the lumen.

LUMEN ECCENTRICITY. (maximum lumen diameter minus minimum lumen diameter) divided by maximum lumen diameter.

LUMEN AREA STENOSIS. (Reference lumen CSA minus minimum lumen CSA) divided by reference lumen CSA. The reference segment used should be specified (proximal, distal, largest, or average—see above). Post-intervention (if dissection is present), it is important to state whether the lumen area is the true lumen or a combination of the true and false lumens.”

IEM measurements. For plaques in which the IEM can be identified, the preceding lumen measurements can be made for the IEM, including the IEM CSA. In addition, the following measurements, modified from the JACC IVUS Consensus Document can be made for plaques in which the IEM can be identified:

PLAQUE (OR ATHEROMA) CSA. The IEM CSA minus the lumen CSA.

MAXIMUM PLAQUE (OR ATHEROMA) THICKNESS. The largest distance from the intimal leading edge to the IEM along any line passing through the center of mass of the lumen.

MINIMUM PLAQUE (OR ATHEROMA) THICKNESS. The shortest distance from intimal leading edge to the IEM along any line passing through the luminal center of mass.

PLAQUE (OR ATHEROMA) ECCENTRICITY. (Maximum plaque thickness minus minimum plaque thickness) divided by maximum plaque thickness.

PLAQUE (OR ATHEROMA) BURDEN. Plaque CSA divided by the IEM CSA. The atheroma burden is distinct from the luminal area stenosis. The former represents the area within the IEM occupied by atheroma regardless of lumen compromise. The latter is a measure of luminal compromise relative to a reference lumen analogous to the angiographic diameter stenosis.

REMODELING. An index of remodeling can be assessed per the JACC IVUS Consensus Document, modified for the IEM (lesion IEM CSA/reference IEM CSA).

It should be noted that the aforementioned IEM measurements can also be measured for the EEM, if it is identified in the IVOCT image. It is therefore recommended that when reporting these measurements, the use of either IEM or EEM be clearly specified. These measurements furthermore should not be made in cross-sectional images that contain artifacts that obscure a significant portion ($> 90^\circ$) of the image or over regions that contain side branches.

Plaque, plaque component, and thrombus measurements. Plaque components including fibrous tissue, lipid pool, necrotic core, cap, calcium, and macrophage accumulations are segmented or outlined by procedures described in the Online Supplementary Material.

ANGLE. Arc measured using the center of mass of the lumen as the angle point.

DEPTH. The distance between the lumen and the leading edge of the plaque feature.

THICKNESS. The thickest distance between the inner and outer surfaces of the plaque component (valid only if the deep boundary can be identified).

AREA. The CSA of the plaque component (valid only if the deep boundary can be identified).

CAP THICKNESS. Defined as the thickness of a cap present over IVOCT-delineated calcium or necrotic core. Although studies have been performed to compare the IVOCT measurement of fibrous cap thickness with histologic measurements of cap thickness, it was generally considered that this area needs further validation, as the boundary between the cap and the necrotic core is not always straightforward to precisely determine.

MACROPHAGE ACCUMULATION MEASUREMENTS. Quantitative measurements of the high signal and heterogeneity of macrophage accumulations have been estimated using a parameter termed the *normalized standard deviation* (13). Care must be taken to smooth out speckle noise before applying this parameter. Limitations of this parameter include the fact that tissue without macrophages have a non-zero normalized standard deviation because of the inherent tissue microstructure. The capability of IVOCT to visualize macrophage accumulations and other inflammatory components in the vicinity of stent struts has not been documented.

Stent Measurements

Within stented segments, IVOCT allows for measurements that are analogous to IVUS. Although the IVUS approach is valid in principle, IVOCT measurements in practice differ as follows: 1) The IVOCT stent measurement field is at a relatively early stage; 2) IVOCT stent measurements can be more demanding due to the greater amount of microstructural detail visible by IVOCT; 3) a variety of methods are currently used; and 4) the clinical significance of some IVOCT-derived stent measurements is unknown. As a result of these differences, it has been recommended that the IWG-IVOCCT continue to deliberate and document stent measurement methods until comprehensive consensus methodology is uniformly agreed upon. Parameters described next represent consensus definitions at the time of publication of this document.

Stent area measurements. Consensus IVOCT quantitative stent area measurements follow that of the JACC IVUS Consensus Document, modified in part here:

STENT CSA. The area bounded by the stent border.

MINIMUM STENT DIAMETER. The shortest diameter through the center point of the stent.

MAXIMUM STENT DIAMETER. The longest diameter through the center point of the stent.

STENT ECCENTRICITY. (Maximum stent diameter minus minimum stent diameter) divided by maximum stent diameter.

STENT CSA STENOSIS (STENT PERCENT AREA OBSTRUCTION, NEOINTIMA BURDEN). (Stent CSA minus lumen CSA)/stent CSA.

IEM NEOINTIMAL AREA. (IEM CSA minus lumen CSA)/IEM CSA. This parameter can only be defined when the IEM can be delineated.

Stent strut measurements. STRUT MALAPPPOSITION DISTANCE. Distance between the abluminal surface of the strut and the luminal surface of the artery wall. Some investigators have estimated the location of the abluminal surface of the strut by drawing a line from the luminal surface of the strut toward the artery wall, where the line has a length that is equivalent to the known strut plus polymer (if present) thickness. The end of this line is an estimate of the location of the abluminal surface

of the strut. If it is separated abuminally from the luminal contour of the vessel, the strut is considered to be malapposed.

OCT STRUT COVERAGE THICKNESS. Distance between the luminal surface of the covering tissue and the luminal surface of the strut. IVOCT is capable of measuring the tissue overlying a strut within the resolution of the OCT system. The biological and clinical significance of OCT strut tissue coverage thickness that is measured to be less than, equal to, or near the axial resolution of the OCT system is not well understood.

PERCENTAGE OF UNCOVERED STENT STRUTS. The number of struts without distinct overlying tissue, in which the luminal reflection of the strut surface is directly interfacing with the lumen, divided by total number of analyzable struts. This assessment is limited by the axial resolution of the IVOCT system and by blooming artifacts, which can be pronounced with metallic stents.

Length and Volume Measurements

Methodologies for measuring length and volume in IVOCT is presented in the Online Supplementary Material.

IVOCT Validation

Methods for validating IVOCT image interpretation criteria and quantitative measurements are important for future application of this technology. Recommendations for ex vivo, animal model, and phantom validation and correlation with other imaging modalities are presented in the Online Supplementary Material.

Specialized Techniques

A description of specialized OCT techniques, including polarization-sensitive OCT and Doppler OCT, is provided in the Online Supplementary Material.

Reporting of IVOCT Studies

Reporting of IVOCT studies closely follows that recommended in the JACC IVUS Consensus Document, as described in the Online Supplementary Material.

Acknowledgments

The IWG-IVOCT organizers would like to thank Gary Mintz, Maria Radu, Mireille Rosenberg, Gijs van Soest, Junya Shite, and Atsushi Tanaka for their extensive contribution to the IWG-IVOCT and this document. The IWG-IVOCT organizers would like to acknowledge Tom Adriaenssens, Marco Costa, Nate Kemp, Nieves Gonzalo, Giulio Guagliumi, Sergio Waxman, and Giora Weisz for providing images. We would like to thank Tom Probasco, the IVOCT DICOM subgroup, and NEMA WG-01 for nurturing the IVOCT DICOM supplement 151 to ratification. The authors would like to posthumously thank Dr. Don Baim for his support, mentorship, and inspiration. They also would like to express our appreciation for Mike Klimas for his key contributions in helping to initiate and

sustain this effort. Finally, they would like to thank the IWG-IVOCT participants from the pharmaceutical and stent industry for their interest and support and the OCT manufacturers (St. Jude Medical/LightLab, Terumo Corp., and Volcano Corp.) for their collaboration.

Reprint requests and correspondence. Dr. Guillermo J. Tearney, Wellman Center for Photomedicine, Massachusetts General Hospital, BAR703, Boston, Massachusetts 02114. E-mail: gtearney@partners.org.

REFERENCES

1. Mintz GS, Nissen SE, Anderson WD, et al. American College of Cardiology Clinical Expert Consensus Document on Standards for Acquisition, Measurement and Reporting of Intravascular Ultrasound Studies (IVUS). A report of the American College of Cardiology Task Force on Clinical Expert Consensus Documents. *J Am Coll Cardiol* 2001;37:1478–92.
2. Virmani R, Kolodgie FD, Burke AP, Farb A, Schwartz SM. Lessons from sudden coronary death: a comprehensive morphological classification scheme for atherosclerotic lesions. *Arterioscler Thromb Vasc Biol* 2000;20:1262–75.
3. Huang D, Swanson EA, Lin CP, et al. Optical coherence tomography. *Science* 1991;254:1178–81.
4. Barlis P, Gonzalo N, Di Mario C, et al. A multicentre evaluation of the safety of intracoronary optical coherence tomography. *EuroIntervention* 2009;5:90–5.
5. Takarada S, Imanishi T, Liu Y, et al. Advantage of next-generation frequency-domain optical coherence tomography compared with conventional time-domain system in the assessment of coronary lesion. *Catheter Cardiovasc Interv* 2010;75:202–6.
6. Imola F, Mallus MT, Ramazzotti V, et al. Safety and feasibility of frequency domain optical coherence tomography to guide decision making in percutaneous coronary intervention. *EuroIntervention* 2010;6:575–81.
7. Virmani R, Burke AP, Farb A, Kolodgie FD. Pathology of the vulnerable plaque. *J Am Coll Cardiol* 2006;47:C13–8.
8. Templin C, Meyer M, Muller MF, et al. Coronary optical frequency domain imaging (OFDI) for in vivo evaluation of stent healing: comparison with light and electron microscopy. *Eur Heart J* 2010;31:1792–801.
9. Ormiston JA, Serruys PW, Regar E, et al. A bioabsorbable everolimus-eluting coronary stent system for patients with single de-novo coronary artery lesions (ABSORB): a prospective open-label trial. *Lancet* 2008;371:899–907.
10. Gonzalo N, Garcia-Garcia HM, Serruys PW, et al. Reproducibility of quantitative optical coherence tomography for stent analysis. *EuroIntervention* 2009;5:224–32.
11. Terashima M, Rathore S, Suzuki Y, et al. Accuracy and reproducibility of stent-strut thickness determined by optical coherence tomography. *J Invasive Cardiol* 2009;21:602–5.
12. Okamura T, Gonzalo N, Gutierrez-Chico JL, et al. Reproducibility of coronary Fourier domain optical coherence tomography: quantitative analysis of in vivo stented coronary arteries using three different software packages. *EuroIntervention* 2010;6:371–9.
13. Tearney GJ, Yabushita H, Houser SL, et al. Quantification of macrophage content in atherosclerotic plaques by optical coherence tomography. *Circulation* 2003;107:113–9.

Key Words: atherosclerosis ■ consensus document ■ coronary artery ■ intravascular ultrasound ■ optical coherence tomography.

APPENDIX

Expanded information for this article, including the Online Supplementary Material, additional tables, figures, technical glossary, figure credits, and a list of Writing Committee members with their affiliations and relationships with industry, are online.

Update

Journal of the American College of Cardiology

Volume 59, Issue 18, 1 May 2012, Page 1662

DOI: <https://doi.org/10.1016/j.jacc.2012.03.015>

CORRECTIONS

Tearney GJ, Regar E, Akasaka T, et al. Consensus Standards for Acquisition, Measurement, and Reporting of Intravascular Optical Coherence Tomography Studies: A Report From the International Working Group for Intravascular Optical Coherence Tomography Standardization and Validation. *J Am Coll Cardiol* 2012;59:1058–72.

“In preliminary registries of patients imaged with FD-OCT, the most frequent events were transient T-wave inversion or ST segment depression, observed in 10% of cases (6).”

should have read

“In a preliminary registry of patients imaged with FD-OCT, no ischemic ECG changes were noted (6).”

The author Darius Dudeck, MD, should have read Darius Dudek, MD.

The author Erlin Falk, MD, should have read Erling Falk, MD.

The author Hector Garcia, MD, should have read Hector M. Garcia-Garcia, MD.

The author Shinjo Sonada, MD, should have read Shinjo Sonoda, MD, PhD.

The author Thim Troels, MD, PhD, should have read Troels Thim, MD, PhD.

The author Gerrit-Ann van Es, PhD, should have read Gerrit-Anne van Es, PhD.

The authors apologize for these errors.

doi:10.1016/j.jacc.2012.03.015

Hillis LD, Smith PK, Anderson JL, et al. 2011 ACCF/AHA Guideline for Coronary Artery Bypass Graft Surgery: Executive Summary: A Report of the American College of Cardiology Foundation/American Heart Association Task Force on Practice Guidelines (*J Am Coll Cardiol* 2011;59:2584–614; doi:10.1016/j.jacc.2011.08.008).

In Section 4.10.3, Central Nervous System Monitoring, in Class IIb recommendation #1, references 449–451 should be replaced by the following references, which should be added to the References section:

316a. Avidan MS, Zhang L, Burnside BA, et al. Anesthesia awareness and the bispectral index. *N Engl J Med*. 2008;358:1097–108.

316b. Hemmerling TM, Olivier JF, Basile F, et al. Bispectral index as an indicator of cerebral hypoperfusion during off-pump coronary artery bypass grafting. *Anesth Analg*. 2005;100:354–6.

316c. Myles PS, Leslie K, McNeil J, et al. Bispectral index monitoring to prevent awareness during anaesthesia: the B-Aware randomised controlled trial. *Lancet*. 2004;363:1757–63.

References 449–451 should be deleted from the References section. These changes are for concordance with the full-length guideline article (*J Am Coll Cardiol* 2011;58:e123–e210; doi:10.1016/j.jacc.2011.08.009).

doi:10.1016/j.jacc.2012.03.022